

Identification of Genes Uniquely Involved in Frequent Microsatellite Instability Colon Carcinogenesis by Expression Profiling Combined with Epigenetic Scanning

Yuriko Mori,¹ Jing Yin,¹ Fumiaki Sato,² Anca Sterian,¹ Lisa A. Simms,³ Florin M. Selaru,¹ Karsten Schulmann,¹ Yan Xu,¹ Andreea Olaru,¹ Suna Wang,¹ Elena Deacu,¹ John M. Abraham,¹ Joanne Young,³ Barbara A. Leggett,³ and Stephen J. Meltzer¹

Departments of ¹Medicine, Division of Gastroenterology and ²Pathology, University of Maryland School of Medicine and Greenebaum Cancer Center and Baltimore Veterans Affairs Hospital, Baltimore, Maryland, and ³Conjoint Gastroenterology Laboratory, Queensland Institute of Medical Research, Herston, Queensland, Australia.

ABSTRACT

Gene silencing through CpG island hypermethylation has been associated with genesis or progression of frequent microsatellite instability (MSI-H) cancers. To identify novel methylation sites unique to MSI-H colon cancers in an unbiased fashion, we conducted a global expression profiling-based methylation target search. We identified 81 genes selectively down-regulated in MSI-H cancers using cDNA microarray analysis of 41 primary colon cancers. Forty six of these 81 genes contained CpG islands overlapping their 5' untranslated regions. Initial screening of six genes in 57 primary colon cancers detected the following gene with MSI-H cancer-specific hypermethylation: *RAB32*, a *ras* family member and A-kinase-anchoring protein, was methylated in 14 of 25 (56%) MSI-H cancers but in none of 32 non-MSI-H cancers or 23 normal colonic specimens. *RAB32* hypermethylation correlated with *RAB32* mRNA down-regulation and with *hMLH1* hypermethylation. In addition, the *protein-tyrosine phosphatase receptor type O* gene, *PTPRO*, was frequently methylated in right-sided tumors. This methylation screening strategy should identify additional genes inactivated by epigenetic silencing in colorectal and other cancers.

INTRODUCTION

MSI-H colon cancer, a tumor subset defined by defective DNA mismatch repair, is distinguished by clinical characteristics including poor differentiation, severe inflammatory cell infiltration, proximal anatomical location, and a better prognosis (1, 2). The molecular carcinogenetic pathway underlying MSI-H cancers is distinct from the chromosomal instability pathway underlying non-MSI-H cancers (1), resulting in a unique molecular profile (3). One major factor defining the MSI carcinogenetic pathway is a unique set of tumor suppressor genes, including *TGFBR2*, *BAX*, and others, that are inactivated through frameshift mutation at coding region mononucleotide repeats (4, 5). Another distinguishing characteristic of these tumors is the CpG island hypermethylation-mediated silencing of *hMLH1*, one of the essential components of the DNA mismatch repair system (6). CpG island hypermethylation occurring at promoter regions is frequently associated with transcriptional repression and loss of gene function (7). The significance of altered global CpG island methylation patterns in colonic carcinogenesis is under investigation (8, 9). It is possible that hypermethylation-mediated silencing of a subset

of tumor-related genes contributes to the unique molecular phenotype of MSI-H cancers. To identify novel genes inactivated through promoter region CpG island hypermethylation in MSI-H colon cancers, we conducted a comprehensive search of promoter region CpG island hypermethylation using a differential gene expression-based approach.

MATERIALS AND METHODS

Tissues and Cell Lines. Eighty-five primary colon cancers (27 MSI-H and 58 non-MSI-H), 14 colon cancer cell lines (5 MSI-H and 9 non-MSI-H), 26 normal colon mucosae, and 4 normal peripheral WBCs from our tissue repository were used for this study. Extractions of genomic DNAs and total RNAs from frozen samples were performed according to standard protocols. Tumor microsatellite instability (MSI) status was determined based on 11 microsatellite markers; *i.e.*, specimens with MSI at $\geq 30\%$ of informative loci were labeled as MSI-H, whereas specimens showing MSI at $< 30\%$ of informative loci were labeled as non-MSI-H. The primer sequences for these 11 loci are listed in Supplemental Table 1. The assignment of cases to each experiment was based on the quantity and quality of nucleic acids for each specimen. Three MSI-H and three non-MSI-H primary cancers used for the microarray experiments were also included in the real-time quantitative methylation-specific PCR (rtQMSP) experiments. Similarly, four MSI-H and 11 non-MSI-H primary cancers in addition to five normal colon mucosae in the rtQMSP experiments were also included in the real-time quantitative reverse transcription-PCR (rtQRT-PCR) experiments. The clinicopathological characteristics of the cases are summarized in Table 1.

cDNA Microarray Analyses and Significance Analysis of Microarray (SAM) Data. cDNA microarray analysis and preprocessing of raw data were performed as described previously (3). In brief, 30 μg of total RNA were amplified using a T7-based protocol, and 6 μg of the resulting amplified RNA were labeled with Cy3- or Cy5-labeled dCTP. An amplified RNA pool of human cancer cell lines was used as the reference probe (3). In-house microarray slides containing 8064 sequence-verified human cDNA were used (3). We included in our final analysis only 6242 clones with expression information for at least 96% of the tumors. Global intensity-based normalization was performed by a robust scatter-plot smoothing method (3). We performed SAM on the normalized microarray data to select genes differentially expressed between MSI-H and microsatellite-stable cancers at a false discovery rate of < 0.1 .

rtQMSP. rtQMSP was performed using the TaqMan system as described previously (10). In brief, bisulfite treatment of genomic DNAs was performed according to the protocol of J. P. Issa.⁴ A TaqMan primer-probe set to detect the fully methylated allele for each gene was designed within a CpG island overlapping the 5' untranslated region. To normalize data, duplex PCR with an β actin (*ACTB*) primer and probe sequences containing no CpGs was performed. The detailed PCR protocol is described in Supplemental Method 1. CpGenome Universal Methylated DNA (Intergen) was used as a control DNA to generate a standard curve. The ratios for methylated alleles representing the percentage of densely methylated DNA in the sample at the target sequence were calculated as follows:

$$\text{Ratio for methylated allele} = \frac{(TarS/TarC)}{(ActS/ActC)}$$

Received 11/9/03; revised 2/17/04; accepted 2/17/04.

Grant support: This research was supported by Public Health Service awards CA95323, CA098450, CA01808, CA77057, and CA85069, and by the Office of Medical Research, Department of Veterans Affairs.

The costs of publication of this article were defrayed in part by the payment of page charges. This article must therefore be hereby marked *advertisement* in accordance with 18 U.S.C. Section 1734 solely to indicate this fact.

Note: Supplementary data for this article are available at Cancer Research Online (<http://cancerres.aacrjournals.org>).

Requests for reprints: Stephen J. Meltzer, 655 West Baltimore Street, BRB 8-009, Baltimore, Maryland 21201. Phone: (410) 706-3375; Fax: (410) 706-1099; E-mail: smeltzer@medicine.umaryland.edu and Yuriko Mori, 655 West Baltimore Street, BRB 8-012, Baltimore, Maryland 21201. Phone: 1(410) 706-3375; Fax: (410) 706-1099; E-mail: ymori001@umaryland.edu.

⁴ <http://www3.mdanderson.org/leukemia/methylation/bisulfite.html>.

Table 1 Characteristics for the specimens used in each experiment

Experiment		Microarray			rtQMSP ^a				rtQRTPCR				<i>P</i> ^b
		Primary colon tumors			Primary colon tumors			Normal colon (<i>n</i> = 23)	Primary colon tumors			Normal colon (<i>n</i> = 8)	
		H (<i>n</i> = 12)	Non-H (<i>n</i> = 29)	Total (<i>n</i> = 57)	H (<i>n</i> = 25)	Non-H (<i>n</i> = 32)	Total (<i>n</i> = 57)		H (<i>n</i> = 4)	Non-H (<i>n</i> = 11)	Total (<i>n</i> = 15)		
Tissue category													
Age	Mean	67.9	68.6	68.4	70.1	67.2	68.5	67.9	61.0	64.6	63.1	64.8	Microarray: 0.2003 rtQMSP: 0.2518 (Student's <i>t</i> -test)
	Max.	90.0	91.0	91.0	90.0	82.0	90.0	83.0	67.0	79.0	79.0	70.0	
	Min.	36.0	49.0	36.0	52.0	44.0	44.0	51.0	52.0	44.0	44.0	56.0	
	S.D.	14.2	10.2	11.3	9.3	9.3	9.3	8.8	7.0	9.6	8.9	6.1	
Site ^c	NA	0	0	0	0	2	2	8	0	1	1	4	Microarray: 0.0012 rtQMSP: 0.0046 (Fisher's exact test)
	L	1	18	19	5	17	22		1	4	5		
	R	11	10	21	18	11	29		3	5	8		
	NA	0	1	1	2	4	6		0	2	2		
Dukes stage	A	2	1	3	3	2	5		1	0	1		Microarray: 0.1754 rtQMSP: 0.0602 (Mann-Whitney's test)
	B	7	16	23	13	11	24		0	3	3		
	C	3	7	10	7	6	13		2	3	5		
	D	0	4	4	2	10	12		1	3	4		
	NA	0	1	1	0	3	3		0	2	2		
Histological differentiation	WD	0	0	0	0	3	3		0	2	2		Microarray: <0.0001 rtQMSP: 0.0016 (Mann-Whitney's test)
	MD	2	24	26	11	22	33		0	7	7		
	MPD	2	3	5	2	3	5		1	1	2		
	PD	7	1	8	10	2	12		2	0	2		
	NA	1	1	1	2	2	4		1	1	2		

^a rtQMSP, real-time quantitative MSP; rtQRTPCR, real-time quantitative reverse transcription PCR; NA, not available; H, non-H, non-MSI-H; L, left-sided; R, right-sided; WD, well differentiated; MD, moderately differentiated; MPD, moderately to poorly differentiated; PD, poorly differentiated.

^b *P* for the comparison of H vs. non-H primary tumors in each experiment. *P* for rtQRTPCR experiment was not calculated due to the small number of the specimens.

^c Tumors at transverse colon without detailed description on their position were labeled as NA.

where *TarS* and *TarC* represent levels of target gene methylation in the sample and the control DNA, respectively, and *ActS* and *ActC* correspond to the amplified *ACTB* level in the sample and the control DNA, respectively. Specimens with a methylated allele ratio ≥ 0.2 were classified as positive for methylation. Primer and probe sequences are listed in Supplemental Table 1.

rtQRTPCR. rtQRTPCR was performed using the TaqMan system, as described previously (10). The template cDNA for each reaction was synthesized from 500 ng of total RNA using SuperScript III kit (Invitrogen) and random hexamer. TaqMan rRNA Control Reagents (Applied Biosystems) were used for normalization of the data. The detailed PCR protocol is described in Supplemental Method 1. cDNA from a colon cancer cell line was used as the quantification standard. The expression index was calculated according to the following formula for the relative expression of target mRNA:

$$\text{Expression index} = (TarS/TarC)/(rRNAS/rRNAC)$$

where *TarS* and *TarC* represent levels of mRNA expression for the target gene in the sample and control cDNA, respectively, whereas *rRNAS* and *rRNAC* correspond to the amplified rRNA levels in the sample and control cDNA, respectively. The sequences of primers and probes are listed in Supplemental Table 1.

RESULTS

To identify novel targets of hypermethylation-mediated gene silencing in MSI-H colon cancers, we used an approach based on comprehensive scanning of differential gene expression using cDNA microarrays. Initially, we performed a microarray analysis of 12 MSI-H and 29 non-MSI-H primary colon cancers to identify genes significantly down-regulated in MSI-H cancers. Significant down-regulation in MSI-H relative to non-MSI-H cancers was detected by SAM in 81 of 8064 human cDNA clones on our microarrays (Supplemental Table 2). Next, an on-line public database search revealed that 46 of these 81 genes had CpG islands overlapping their 5'-untranslated region or the first exon.⁵ Thus, 46 genes were potential targets of hypermethylation-mediated gene silencing unique to MSI-H colon cancers.

We analyzed the methylation status of CpG islands overlapping the 5'-untranslated regions of six genes selected from these 46 genes based

on putative functional links to human cancers: *EFNB1*, *ITPR2*, *HDAC11*, *PTPRO*, *RAB32*, and *SDBCAG84*. A rtQMSP assay was performed on 13 primary colon cancers (five MSI-H and eight non-MSI-H), and methylation in tumors was detected in two of the six genes. These two genes, *PTPRO* and *RAB32*, were analyzed further in a larger number of samples consisting of 57 primary cancers, 14 colon cancer cell lines, 23 normal mucosae, and four normal peripheral WBCs. Hypermethylation of *RAB32*, a *Ras* family member that encodes a mitochondrial A-kinase-anchoring protein, was detected in an MSI-H cancer-specific manner; *i.e.*, *RAB32* was methylated in 14 (56%) of 25 MSI-H primary cancers but in none of 32 non-MSI-H primary cancers (Fig. 1A; $P < 0.00001$ by Fisher's exact test and Student's *t* test). Similarly, *RAB32* methylation was found in four of five (80%) MSI-H cell lines but in only one (11%) of nine non-MSI-H cell lines. No *RAB32* methylation was detected in either 23 normal mucosae or four normal peripheral WBCs. *PTPRO*, a membranous protein tyrosine phosphatase gene, was frequently methylated in a tumor-specific manner. *PTPRO* methylation was detected in 28 of 55 (55%) primary cancers but in none of 18 normal mucosae (Fig. 1B; $P = 0.00003$ by Fisher's exact test and $P = 0.0022$ by Student's *t* test). *PTPRO* hypermethylation was more frequent in MSI-H primary cancers (16 of 25, 64%) than in non-MSI-H primary cancers (12 of 30, 40%), but the difference between these two tumor subgroups was not significant.

We further investigated the association between hypermethylation and silenced mRNA expression for *RAB32* and *PTPRO*. rtQRTPCR analyses were performed on 14 primary cancers (3 MSI-H and 11 non-MSI-H), 14 cell lines (five MSI-H and nine non-MSI-H), and eight normal mucosae. All eight normal mucosae expressed *RAB32* mRNA. MSI-H cancers tended to show lower *RAB32* expression than did non-MSI-H cancers and normal colon mucosae, and the results from microarray and rtQRTPCR matched closely among five primary cancers (two MSI-H and three non-MSI-H) analyzed by both methods (data not shown). All five cell lines with *RAB32* methylation lacked mRNA expression, and both MSI-H primary cancers with *RAB32* methylation showed the lowest mRNA levels among tissue specimens analyzed (data not shown). Fig. 2 illustrates the inverse association between methylation and mRNA expression of the *RAB32* gene; *i.e.*, *RAB32* mRNA expression was more significantly down-regulated in

⁵ University of California at Santa Cruz Human Genome Browser: <http://genome.ucsc.edu/cgi-bin/hgGateway>.

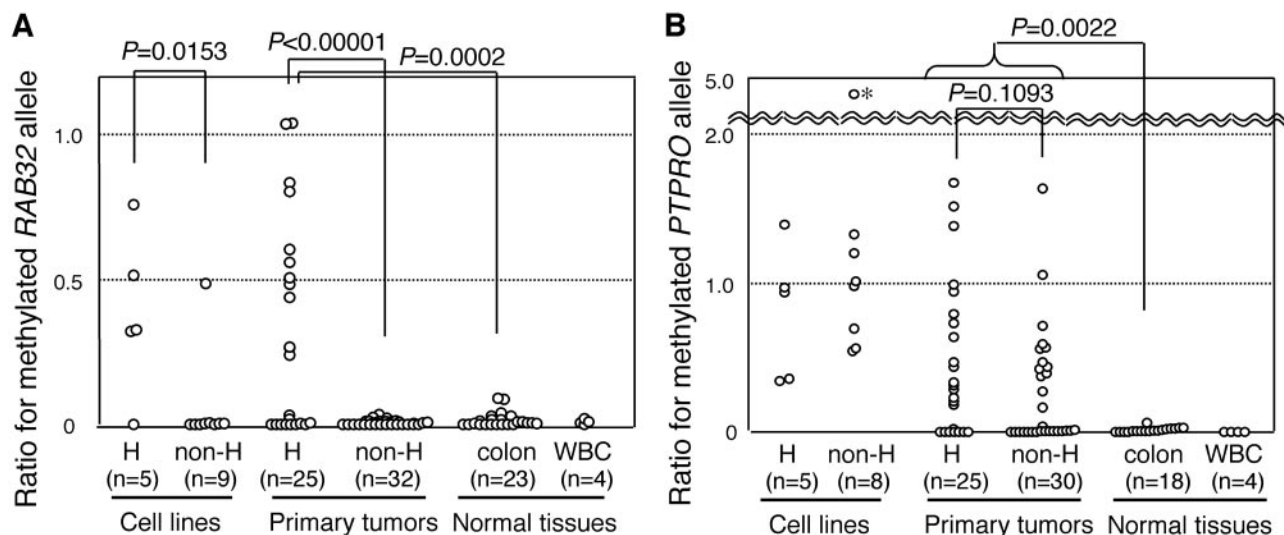


Fig. 1. Methylation levels for *RAB32* and *PTPRO* in association with the sample MSI status. These one-dimensional scatter plots show methylated allele ratios of *RAB32* (A) or *PTPRO* (B) in various sample subtypes; H, MSI-H; non-H, non-MSI-H. Ratio for methylated allele was the ratio of the relative quantities of fully methylated genomic DNA for the target gene to the *ACTB* genomic DNA. The primer and TaqMan probe set for *ACTB* does not contain any CpGs and amplifies the sample regardless of the methylation status. A chemically modified fully methylated human genomic DNA was used as the quantification standard. All *P*s were calculated by Student's *t* test. A, *RAB32* was methylated only in MSI-H tumors, with one exception of a non-MSI-H cancer cell line. B, only cancerous specimens had *PTPRO* methylation. Tumor MSI status did not show any significant association with the *PTPRO* methylation level. The dot marked with an asterisk represents a non-MSI-H colon cancer cell line colo205, which had an extremely high methylated allele ratio (4.56).

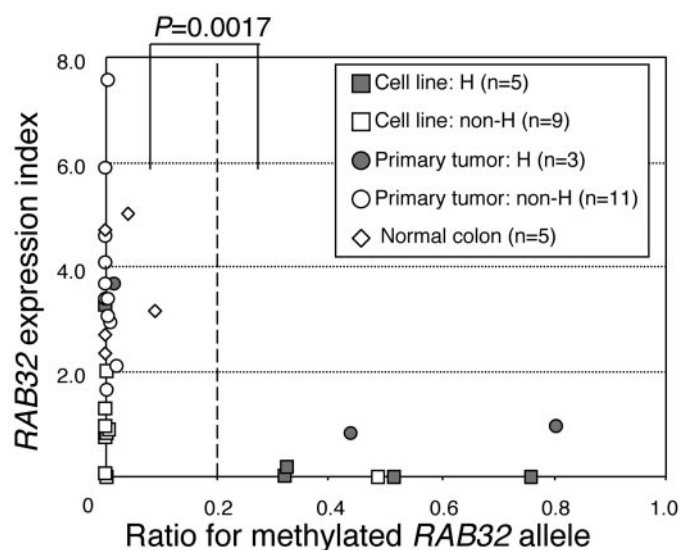


Fig. 2. *RAB32* mRNA expression levels in association with sample microsatellite instability (MSI) status or *RAB32* methylation ratio for the specimens. This two-dimensional scatter plot shows inverse association between levels of methylation (X-axis) and mRNA expression (Y-axis) of *RAB32*. *RAB32* expression index is a representative value of the relative *RAB32* mRNA expression level standardized by the rRNA quantity. A non-MSI-H colon cancer cell line WiDr was used as the quantification standard specimen. A square represents each cell line, a circle represents each primary tumor, and a diamond represents each normal colon specimen. MSI-status of the specimens are indicated by the color of the symbol (gray symbols are MSI-H and open symbols are non-MSI-H). *RAB32* mRNA expression was significantly lower in specimens with *RAB32* methylation (ratio for methylated allele ≥ 0.2) than in specimens without *RAB32* methylation (methylated allele ratio < 0.2) with the *P* of 0.0017 (Student's *t* test).

specimens with *RAB32* hypermethylation than in specimens without *RAB32* hypermethylation ($P = 0.0017$; Student's *t* test). In accordance with our microarray results, *PTPRO* mRNA expression levels also tended to be lower in MSI-H primary cancers than in non-MSI-H primary cancers (data not shown), and microarray and rtQRT-PCR results matched closely in six primary cancers (three MSI-H and three non-MSI-H) analyzed by both methods (data not shown). However, *PTPRO* mRNA expression was very low or absent in normal colonic

specimens and showed no significant association with *PTPRO* methylation ($P = 0.7354$; Student's *t* test; data not shown).

RAB32 hypermethylation was then analyzed for its association with clinicopathological and molecular characteristics of tumors. One of our major interests was to analyze *RAB32* hypermethylation in association with *hMLH1* hypermethylation, the cause of MSI in the majority of sporadic MSI-H cancers. As shown in Table 2, *RAB32* hypermethylation occurred only in specimens with *hMLH1* hypermethylation. Furthermore, *RAB32* hypermethylation occurred only in tumors with *hMLH1* hypermethylation, and levels of hypermethylation of *RAB32* and *hMLH1* showed a significant linear correlation in 25 MSI-H primary colon cancers (correlation coefficient, 0.907; $P < 0.0001$). *RAB32* hypermethylation in MSI-H primary cancers was also significantly associated with right-sided tumor location ($P = 0.0038$, Fisher's exact test). On the other hand, *RAB32* hypermethylation was not associated with histological differentiation, tu-

Table 2. *RAB32* methylation status of 25 primary MSI-H colon cancers in association with their case or tumor characteristics

Category		RAB32 methylation			<i>P</i>
		(+)	(-)	Total	
<i>hMLH1</i> methylation	(+)	14	1	15	< 0.00001 (Fisher's exact test) correlation coefficient = 0.907 ($P < 0.0001$)
	(-)	0	10	10	
Site ^a	L	0	5	5	0.0038 (Fisher's exact test)
	R	14	4	18	
	NA ^b	0	2	2	
Histological differentiation	WD + MD	4	7	11	0.0635 (Fisher's exact test)
	MPD + PD	9	3	12	
	NA	1	1	2	
Dukes stage	A + B	11	5	16	0.0823 (Fisher's exact test)
	C + D	3	6	9	
Age	≤ 70	6	7	13	0.1906 (Fisher's exact test) correlation coefficient = 0.174 ($P = 0.4095$)
	> 70	8	4	12	

^a Tumors at transverse colon without detailed description on their position were labeled as NA.

^b L, left-sided; R, right-sided; NA, not available; WD, well differentiated; MD, moderately differentiated; MPD, moderately or poorly differentiated; PD, poorly differentiated.

Table 3 *PTPRO* methylation status of 55 primary colon cancers in association with their case or tumor characteristics

Category		PTPRO methylation			P
		(+)	(-)	Total	
MSI status ^a	H	16	9	25	0.0462 (Fisher's exact test)
	non-H	12	18	30	
hMLH1 methylation	(+)	15	3	18	0.0008 (Fisher's exact test) correlation coefficient = 0.634 ($P < 0.0001$)
	(-)	13	24	37	
Site ^b	R	22	7	29	0.00016 (Fisher's exact test)
	L	3	18	21	
	NA	3	2	5	
Histological differentiation ^c	WD + MD	15	20	35	0.0421 (Fisher's exact test)
	MPD + PD	12	5	17	
	NA	1	2	3	
Dukes stage	A + B	18	10	28	0.0275 (Fisher's exact test)
	C + D	9	16	25	
	NA	1	1	2	
Age	≤70	12	19	31	0.0355 (Fisher's exact test) correlation coefficient = 0.152 $P = 0.2753$ (for the linear correlation test)
	>70	15	8	23	
	NA	1	0	1	

^a H, MSI-H; non-H, non-MSI-H.

^b Tumors at transverse colon without detailed description on their position were labeled as NA.

^c R, right-sided; L, left-sided; NA, not available; WD, well differentiated; MD, moderately differentiated; MPD, moderately to poorly differentiated; PD, poorly differentiated.

mor stage, or age. Similarly, Table 3 summarizes correlative analyses of *PTPRO* hypermethylation and tumor characteristics of 55 primary colon cancers (both MSI-H and non-MSI-H). *PTPRO* hypermethylation was significantly associated with right-sided tumor location ($P = 0.00016$; Fisher's exact test) and hMLH1 hypermethylation (correlation coefficient, 0.634; $P < 0.0001$). No associations were observed between *PTPRO* hypermethylation and tumor MSI-status, histological differentiation, Dukes stage, or age.

DISCUSSION

Comprehensive identification of gene silencing through promoter region hypermethylation has proven fruitful not only for a deeper understanding of human carcinogenesis, but also in the development of biomarkers relevant to the clinical care of patients, because hypermethylation of some genes has been reported as a potential biomarker for early detection or prognostication (11, 12). Several methods of global screening for differentially methylated CpG islands have been described previously (13, 14). Although valuable, these methods were not specific to promoter region hypermethylation or hypermethylation accompanied by gene silencing, which should be necessary in order for a biological effect on cancer progression to be exerted. Therefore, a comprehensive survey based on differential mRNA expression offers the advantage of limiting identification of promoter region hypermethylation events to those correlated with gene silencing only (15).

In the current study, we combined methylation target scanning with differentially expressed gene screening by cDNA microarray to identify novel targets of hypermethylation-mediated gene silencing in MSI-H colon cancers. By using this strategy, we identified 46 genes as candidate targets, and a detailed analysis of 6 of these 46 genes successfully identified a novel target of MSI-H tumor-specific hypermethylation that correlated with gene silencing. This novel target, RAB32, is a mitochondrial small molecular weight G-protein that belongs to the Ras superfamily and participates in synchronization of mitochondrial fission (16). RAB32 is distinct from other RAB family proteins by its characteristics as an A-kinase-anchoring protein, *i.e.*, the ability to anchor the cyclic AMP-dependent kinase (PKA) by

binding to the regulatory subunit of PKA (16). Therefore, RAB32 inactivation may alter the phenotype of the cell through disruption or dysregulation of one or more cyclic AMP-PKA-mediated cellular functions in or around mitochondria, including apoptosis and energy production (17, 18).

RAB32 hypermethylation was associated only with MSI-H, or more specifically *hMLH1* promoter region hypermethylation, among all tumor characteristics analyzed in this study. An observed association with right-sided tumor location probably arose from the fact that MSI-H cancers are predominantly right-sided. Aging did not appear to increase the hypermethylation rate for *RAB32*, although aging is known to affect methylation rates of several genes (19). The observed close correlation between *hMLH1* and *RAB32* methylation suggests that cancers caused by *hMLH1* methylation form a subgroup with a slightly different molecular phenotype in MSI-H cancers. A previous report on differences in features between hereditary nonpolyposis colon carcinoma and sporadic MSI-H cancers supports this hypothesis (20). Another molecular abnormality associated with *hMLH1* hypermethylation is activating mutation of *BRAF*, which seems to functionally compensate for the lack of *KRAS* mutation in MSI-H cancers (21, 22). Interestingly, PKA also participates in the RAS/RAF/mitogen-activated protein kinase-extracellular signal-regulated kinase kinase/extracellular signal-regulated kinase cascade as a modulator (23), suggesting that PKA is a potential link between *BRAF* and *RAB32*. Additional functional studies are required to scrutinize the role of *RAB32* in both these signaling pathways and the genesis of human cancers.

The protein tyrosine phosphatase receptor type O gene, *PTPRO*, was another gene displaying frequent tumor-specific hypermethylation but not in an MSI-H-specific manner. Recently, DNA hypermethylation-mediated silencing of *PTPRO* was reported in rat hepatocellular cancers induced by a folic acid-deficient diet (24). In contrast to rat liver, gene silencing by *PTPRO* hypermethylation was not observed in human colon. However, *PTPRO* hypermethylation in colon cancers showed a remarkable association with right-sided tumor location independent of tumor MSI status. Interestingly, diet has been suggested as one of the modifiers of DNA methylation patterns and is known to have a prominent influence on the intraluminal contents of the right hemicolon (25). Thus, *PTPRO* hypermethylation could conceivably constitute a marker of diet-related alterations in colonic methylation pattern.

In summary, we have presented an application of differential expression scanning with cDNA microarrays to the comprehensive identification of promoter region hypermethylation-mediated gene silencing in human cancer. In proof of principle, a novel methylation target specific to MSI-H colon cancers was identified using this approach. This novel target, RAB32, participates in the cyclic AMP-PKA signaling pathway and is potentially relevant to a subset of MSI-H cancer progression. These findings suggest that this combined strategy offers the potential to discover additional methylation events unique to other specific cancer subgroups, and in doing so, to provide insights into the unique biologies underlying these tumor subgroups.

REFERENCES

- Ionov Y, Peinado MA, Malkhosyan S, Shibata D, Perucho M. Ubiquitous somatic mutations in simple repeated sequences reveal a new mechanism for colonic carcinogenesis. *Nature (Lond)* 1993;363:558-61.
- Thibodeau SN, Bren G, Schaid D. Microsatellite instability in cancer of the proximal colon. *Science (Wash D C)* 1993;260:816-9.
- Mori Y, Selaru FM, Sato F, et al. The impact of microsatellite instability on the molecular phenotype of colorectal tumors. *Cancer Res* 2003;63:4577-82.
- Markowitz S, Wang J, Myeroff L, et al. Inactivation of the type II TGF- β receptor in colon cancer cells with microsatellite instability. *Science (Wash D C)* 1995;268:1336-8.

5. Rampino N, Yamamoto H, Ionov Y, et al. Somatic frameshift mutations in the BAX gene in colon cancers of the microsatellite mutator phenotype. *Science (Wash D C)* 1997;275:967–9.
6. Kane MF, Loda M, Gaida GM, et al. Methylation of the hMLH1 promoter correlates with lack of expression of hMLH1 in sporadic colon tumors and mismatch repair-defective human tumor cell lines. *Cancer Res* 1997;57:808–11.
7. Baylin SB, Herman JG. DNA hypermethylation in tumorigenesis: epigenetics joins genetics. *Trends Genet* 2000;16:168–74.
8. Toyota M, Ahuja N, Ohe-Toyota M, Herman JG, Baylin SB, Issa JP. CpG island methylator phenotype in colorectal cancer. *Proc Natl Acad Sci USA* 1999;96:8681–6.
9. Yamashita K, Dai T, Dai Y, Yamamoto F, Perucho M. Genetics supersedes epigenetics in colon cancer phenotype. *Cancer Cell* 2003;4:121–31.
10. Sato F, Shibata D, Harpaz N, et al. Aberrant methylation of the HPP1 gene in ulcerative colitis-associated colorectal carcinoma. *Cancer Res* 2002;62:6820–2.
11. Esteller M, Garcia-Foncillas J, Andion E, et al. Inactivation of the DNA-repair gene MGMT and the clinical response of gliomas to alkylating agents. *N Engl J Med* 2000;343:1350–4.
12. Kawakami K, Brabender J, Lord RV, et al. Hypermethylated APC DNA in plasma and prognosis of patients with esophageal adenocarcinoma. *J Natl Cancer Inst (Bethesda)* 2000;92:1805–11.
13. Toyota M, Ho C, Ahuja N, et al. Identification of differentially methylated sequences in colorectal cancer by methylated CpG island amplification. *Cancer Res* 1999;59:2307–12.
14. Ushijima T, Morimura K, Hosoya Y, et al. Establishment of methylation-sensitive-representational difference analysis and isolation of hypo- and hypermethylated genomic fragments in mouse liver tumors. *Proc Natl Acad Sci USA* 1997;94:2284–9.
15. Yamashita K, Upadhyay S, Osada M, et al. Pharmacologic unmasking of epigenetically silenced tumor suppressor genes in esophageal squamous cell carcinoma. *Cancer Cell* 2002;2:485–95.
16. Alto NM, Soderling J, Scott JD. Rab32 is an A-kinase anchoring protein and participates in mitochondrial dynamics. *J Cell Biol* 2002;158:659–68.
17. Harada H, Becknell B, Wilm M, et al. Phosphorylation and inactivation of BAD by mitochondria-anchored protein kinase A. *Mol Cell* 1999;3:413–22.
18. Papa S, Sardanelli AM, Scacco S, Technikova-Dobrova Z. cAMP-dependent protein kinase and phosphoproteins in mammalian mitochondria. An extension of the cAMP-mediated intracellular signal transduction. *FEBS Lett* 1999;444:245–9.
19. Ahuja N, Li Q, Mohan AL, Baylin SB, Issa JP. Aging and DNA methylation in colorectal mucosa and cancer. *Cancer Res* 1998;58:5489–94.
20. Young J, Simms LA, Biden KG, et al. Features of colorectal cancers with high-level microsatellite instability occurring in familial and sporadic settings: parallel pathways of tumorigenesis. *Am J Pathol* 2001;159:2107–16.
21. Dong J, Phelps RG, Qiao R, et al. BRAF oncogenic mutations correlate with progression rather than initiation of human melanoma. *Cancer Res* 2003;63:3883–5.
22. Rajagopalan H, Bardelli A, Lengauer C, Kinzler KW, Vogelstein B, Velculescu VE. Tumorigenesis: RAF/RAS oncogenes and mismatch-repair status. *Nature (Lond)* 2002;418:934.
23. Stork PJ, Schmitt JM. Crosstalk between cAMP and MAP kinase signaling in the regulation of cell proliferation. *Trends Cell Biol* 2002;12:258–66.
24. Motiwala T, Ghoshal K, Das A, et al. Suppression of the protein tyrosine phosphatase receptor type O gene (PTPRO) by methylation in hepatocellular carcinomas. *Oncogene* 2003;22:6319–31.
25. Ross SA. Diet and DNA methylation interactions in cancer prevention. *Ann N Y Acad Sci* 2003;983:197–207.